

Experimentation on Mechanical properties of Al 7075 reinforced with Hafnium carbide, Silicon nitride, and Molybdenum Disulfide hybrid composites

^[1] N. Ummal Salmaan, ^[2] D. S. Robinson Smart, ^[3] S. Antony Raja

^[1] Research scholar, Department of Mechanical Engineering, Karunya institute of technology and sciences, India, ^[2] Professor, Department of Mechanical Engineering, Karunya institute of technology and sciences, India, ^[3] Associate Professor, Department of Mechanical Engineering, Karunya institute of technology and sciences, India

^[1] ummalsalmaan90@gmail.com, ^[2] smart@karunya.edu, ^[3] santonyraja@karunya.edu.

Abstract:

The objective of the present research is to investigate the Mechanical properties of Hafnium carbide (HfC), Silicon Nitride (Si_3N_4) and Molybdenum Disulfide (MoS_2) reinforced with Al 7075. The secondary particles like Si_3N_4 (2 to 8) wt.% increase in the step of 3%, HfC (0.5 to 2) wt.% increase in the step of 0.75% and MoS_2 (2 to 5) wt.% increase in the step of 1.5 % are reinforced in base material Al7075 alloy using stir casting methodology. The casted specimen is machined using wire cut EDM as per the ASTM standards. Vickers's microhardness test and Ultimate tensile strength were performed; the result indicates Al7075 with 5wt.% Si_3N_4 , 1.25wt.% HfC, 3.5wt.% MoS_2 increases the hardness and tensile strength by indicating excellent mechanical properties, however, adding more reinforcements decreases hardness and tensile strength. The fatigue tests were performed on different specimens based upon the tension-compression cyclic loading, calculated the endurance limit, stress and no failure mode of each specimen by predicting the cut off value at 10^4 cycles; the Al7075 with 5wt.% Si_3N_4 , 1.25wt.% HfC, 3.5wt.% MoS_2 shows maximum stress at 1.6×10^4 Cycles. The SEM analysis after casting shows the disperse of reinforcements with the base alloy, and the fractography analysis of tensile test shows the fracture behaviour of the specimens that show the changes of behaviour from ductile to brittle by adding more reinforcements. The EDS shows the presence of materials based upon the wt.% added.

Index Terms: Al7075, HfC, Si_3N_4 , MoS_2 , Mechanical properties.

1. INTRODUCTION

The old conventional engineering materials are replaced by aluminium composite materials [1]. The Al7075 is a matrix material used in various applications. The researchers are mainly developing the aluminium matrix composites, which have to be light in weight, high strength, and good in wear and corrosion resistance, especially in Automobile and Aerospace applications [2]. The Al7075 matrix material has some disadvantages while used in this automotive application without adding any reinforcements. A substantial improvement in mechanical properties if just 30% of the reinforcements are added to Al7075 metal matrix composites [3]. Adding the hybrid reinforcements has a positive effect on improving the hardness and wear resistance of the alloy composites and improving microhardness and tensile strength while increasing particulate content [4], [5]. Some of the ceramic materials that some researchers have suggested improving the properties of Al7075 are Silicon carbide, Titanium carbide, zirconium carbide, B_4C , and TiB_2 . The Experiment conducted on Al7075 as a base MMC and SiC and B_4C have particulate materials the tensile strength, yield strength increases as the wt.% of SiC and B_4C increases, and the ductile and brittle fracture behaviour shown in the fractographic analysis [6]. To offer high elastic modulus, hardness, low density, the TiC is the most attractive reinforcement with Al7075. The hardness and tensile strength increased as the Experiment

with Al7075, and different wt.% of TiC has added [7]. The ZrO₂ plays a significant role as reinforcements and Aluminium alloy as a base alloy. The Al7075 is fabricated by adding different wt.% of ZrO₂ and shows an immense increase in microhardness, tensile strength and impact strength. Still, the decrease in ductility and fracture toughness [8].

The B₄C and MoS₂ reinforcements with various wt.% is added with Al7075 around 81%, and 4% of hardness and tensile strength is increased based on the particulates added. The Coefficient of friction was also reduced to 63%. It is due to the presence of solid lubricant MoS₂ [9]. When the hard ceramic particle TiB₂ wt.% is kept constant, and Gr wt.% is changed from 2 wt.% to 8 wt.% on the difference of 2%, the hardness and ultimate tensile strength are increased up to 74% and 68% by increasing the Gr, but there is a decrease in ductility due to the inclusion of TiB₂ and Gr [10]. The various manufacturing technique is used to fabricate the Al7075 based alloy matrix along with the reinforcements such as stir casting technique [11], powder metallurgy technique [12], Friction stir casting [13], squeeze casting [14] are the most commonly used manufacturing techniques for fabricating MMC's. The most attractive technique is the powder metallurgy technique due to its advantages in uniform distribution and reduced processing temperature but PM techniques is best for large scale manufacturing. However, stir casting is less expensive. By the stir casting technique, the Al7075 with SiC nanoparticles are heated up to 750°C. The nanoparticles are injected at the preheated stage at 200°C, and then the mechanical stirrer is used to stir up at 250 rpm in the presence of argon gas inert atmosphere shows an increase in the mechanical properties if the densities of the reinforcement and the base alloy have significant differences [15].

So, it is clear that adding up the reinforcements shows good positive results in increasing the mechanical properties and good bonding between matrix and reinforcement material [16]. The present objective of the research work is the preparation of Al7075/Si₃N₄/HfC/MoS₂ Hybrid composite fabricated using stir casting technique, there is a lot of research gap on the hard ceramic particle Hafnium carbide and so, the experiments were performed to investigate the Hardness, Ultimate tensile strength, Fatigue limit and understanding the microstructure formation of the hybrid composite to know the distribution of the reinforcements in the Al7075 base matrix.

2. EXPERIMENT PROCEDURE

The base matrix metal is Al 7075 purchased at (Coimbatore Metal Mart, Coimbatore) which have different chemical compositions, as shown in Table 1. The properties of the reinforcements are given in Table 2. The reinforcements have the particle size of micrometre purchased from (Alpha Aesar, USA). The total amount of the matrix base material and the reinforcements is selected by measuring the volume percentages in Table

Table 1. Chemical Compositions of Al 7075

Element	Zn	Fe	Mn	Cu	Cr	Si	Ti	Mg	Al
Wt.%	2.1	0.4	0.3	1.9	2.9	0.5	0.2	6.2	Bal.

Table 2. Properties of Reinforcements

Properties	Hfc	Si ₃ N ₄	MoS ₂
------------	-----	--------------------------------	------------------

Molar Mass	190.54 g/mol	140.28 g/mol	160.07 g/mol
Density	12.7 g/cm ³	3.17 g/cm ³	5.06 g/cm ³
Melting Point	3890°C	1900°C	1185°C
Boiling Point	4600°C	N/A	450°C
Hardness	2300 kg/mm ²	1450 kg/mm ²	900 kg/mm ²



Fig 1. a) Micro Hardness Tester b) Universal Testing Machine c) Fatigue Testing Machine d) Fatigue test specimen holder

Table 3. wt.% of the Reinforcements

Specimen	Al7075	Si ₃ N ₄	HfC	MoS ₂
C1	100%	-	-	-
C2	-	2 %	0.5 %	2 %
C3	-	5 %	1.25 %	3.5 %
C4	-	8 %	2 %	5 %

*C1- Al7075, C2- Al7075+2wt.% Si₃N₄+0.5wt.% HfC+2wt.% MoS₂, C3- Al7075+5wt.% Si₃N₄+1.25wt.% HfC+3.5wt.% MoS₂, C4- Al7075+8wt.% Si₃N₄+2wt.% HfC+5wt.% MoS₂

2.1. Stir Casting Method:

The composites are all fabricated by the stir casting method. The Al 7075 is a 5mm round rod, and 100mm in length is cut into a small piece to be easy to add inside the furnace. First, the base metal matrix was heated up to 800°C, the reinforcements were added by using the mechanical stirrer; it stirred up manually at a maximum of 200 rpm. Then finally, the melted composite material was transferred to mild steel die 100mm×100mm×10 mm [17].

2.2 Wire cut Electrical Discharge Machining

Then by using the wire EDM machine, the fabricated samples are machined for the required testing as per the ASTM E8 standard guidelines. The distance between the specimen and molybdenum wire is 0.02 mm at a constant controlled by a servo control system having a wire diameter of 18mm and wire feed rate at 4 mm/min [18].

2.3 Hardness

By using the micro hardness tester (Mitutoyo, Japan – HM113) shown in Fig.1a, the Vickers hardness were measured at ten different points using diamond indenter for each ASTM E92 standard specimen at load 0.05 HV the interminable dwell time between every test is 5 secs to avoid the repeatability of the results.

2.4 Tensile Test

The tensile tests were conducted on ASTM E8M04 standard specimen by regulating the tensile strength through Computerized Universal Testing Machine (TMC, Chennai – CUTM) shown in Fig.1b with a strain rate of 1mm/min at a maximum load of 50 kN Fig.2 & Fig.3 shows the standard specimen for hardness and tensile strength.

2.5 Fatigue Test

The computerized fatigue testing machine at (Karunya Institute of Technology, Coimbatore) is used to conduct the fatigue test for the specimens shown in the fig.1c, prepared according to the ASTM E606 standard having a gauge length of 40mm. The gauge point of the fatigue test specimens will undergo a constant surface finish to reduce the bending conditions during testing. The prepared specimens are loaded axially, as shown in Fig.1d with tension-compression cyclic loading to a maximum of 50-60 cycles /min and maximum load of 60 kN with a ratio of stress as $R=0.2$ repeatedly at maximum load until there is a failure in the cycle at the room temperature. maximum 6 samples are used for each specimen from higher stress to lower stress until it exceeds the predetermined number of cycles (10^4).

2.6 SEM

The Scanning Electron Microscopy is used to analyse the distribution of the reinforcements with the base alloy. The SEM fractography of tensile test specimens was studied to understand the nature and cause of the fracture. The Electron Dispersive Spectroscopy (EDS) show the wt.% of the material in each specimen according to the composition (PSGIAS, Coimbatore).

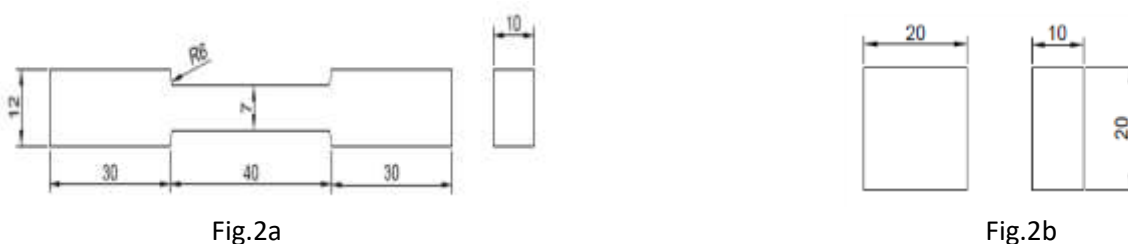


Fig. 2 a) Standard specimen for Tensile test b) Standard specimen for Hardness test

3. RESULTS & DISCUSSION

3.1 Density and porosity

The theoretical and actual density was calculated by the role of mixture and Archimedes' principle. The addition of reinforcement increases the density of composite materials, and also, there will be an increase in the porosity due to the pore nucleation on the particulate surface of the reinforcements. The porosity level should be limited to 4.0 % is acceptable [19]. The porosity percentage of Theoretical and Experimental density is calculated by the given Equation.1 and values shown in Table.4 and the comparison of Theoretical and Experimental density shown in Fig.3

$$\% \text{ of porosity} = \frac{\text{Theoretical Density} \frac{g}{cm^3}}{\text{Experimental Density} \frac{g}{cm^3}} \times 100 \quad (1)$$

Table 4. Comparison of Theoretical, Experimental density and percentage of Porosity

Specimen Composition	Theoretical density (g/cm ³)	Experimental Density (g/cm ³)	% of porosity
Al7075	2.72	2.69	1.102
Al7075+2%Si ₃ N ₄ +0.5%HfC+2%MoS ₂	2.83	2.81	0.70
Al7075+5%Si ₃ N ₄ +1.25%HfC+3.5%MoS ₂	2.89	2.86	1.03
Al7075+8%Si ₃ N ₄ +2%HfC+5%MoS ₂	2.96	2.91	1.68

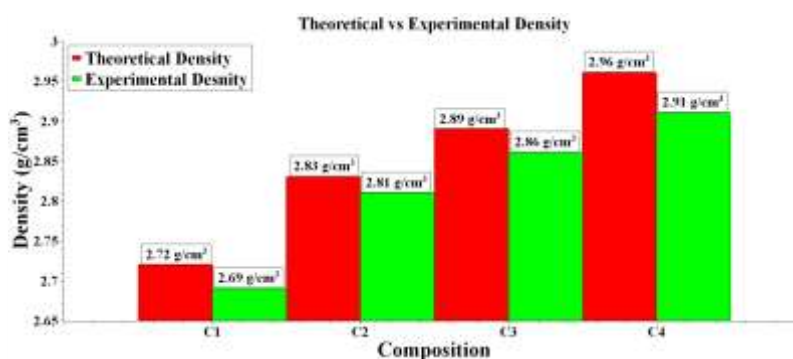


Fig 3. Comparison of Theoretical and Experimental Density

3.2 Evaluation of Hardness Test

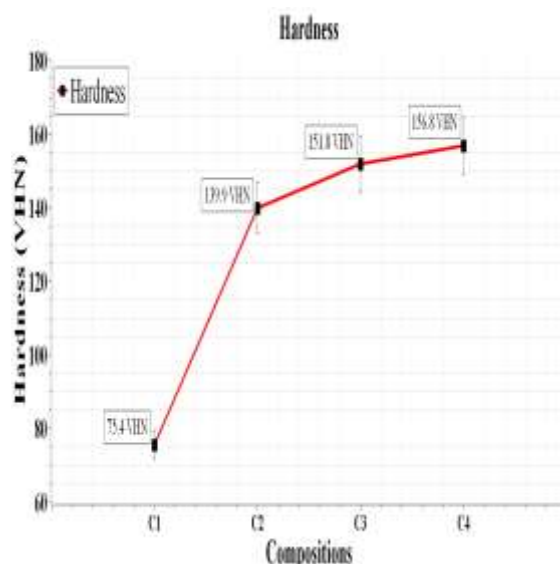


Fig 4. Variation of hardness with different specimen

Fig.4 shows the hardness variation with the different specimens as we can see that the wt.% of the reinforcements increased the hardness value. The pure base metal Al7075 has the lowest hardness value of 75.4 VHN due to the absence of reinforcements; as the reinforcements are added in specimens C2 to C4, the hardness value is increased according to the reinforcement wt. % [20]. It indicates that the Si_3N_4 and HfC ceramic particles are evenly distributed throughout the base metal matrix because the reinforcement particle size ($45\mu\text{m}$) is large when compared to the base matrix particles size ($20\mu\text{m}$) as we can see a 90% increase in hardness as the reinforcements added [21].

3.3 Evaluation of Tensile Strength

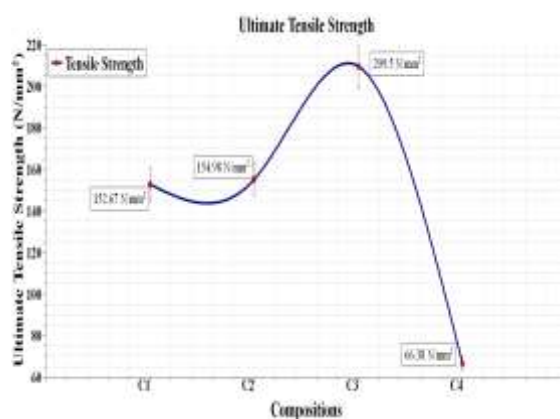


Fig.5 Variation of Tensile Strength with different Specimen

The Fig.5 and Fig.6 show the variation of Tensile strength and % of elongation with the different specimens as we can see that increasing the wt.% of the reinforcement with the base alloy increases the tensile strength from 152.67 N/mm² to 209.5 N/mm² at room temperature. It shows that the properties and structures of the reinforcements control the mechanical properties of the composites where the load distributes and transfers from the matrix, which result in increased elastic

modulus and strength [22]. As the reinforcement wt., % is further increased, the Tensile strength is decreased to the 66.38 N/mm² due to the improper bonding between the base alloy and reinforcements which causes dislocation at the interface. It will also decrease if there is a difference in the coefficient of thermal expansion of base alloy and reinforcements, leading to the diffusion of alloying elements and creating crack nucleation. Furthermore, due to the clustering of reinforcement particles with the matrix [23]. to overcome this dislocation between the interfaces, the Orowan mechanism which used in strengthening the dislocation by creating an agglomeration between particles/matrix interface, creates a dislocation loop to overcome the obstacles between the interfaces by that it increases the characteristic of tensile which leads to dispersion strengthening of the reinforcement particles with the base alloy [24], [25].

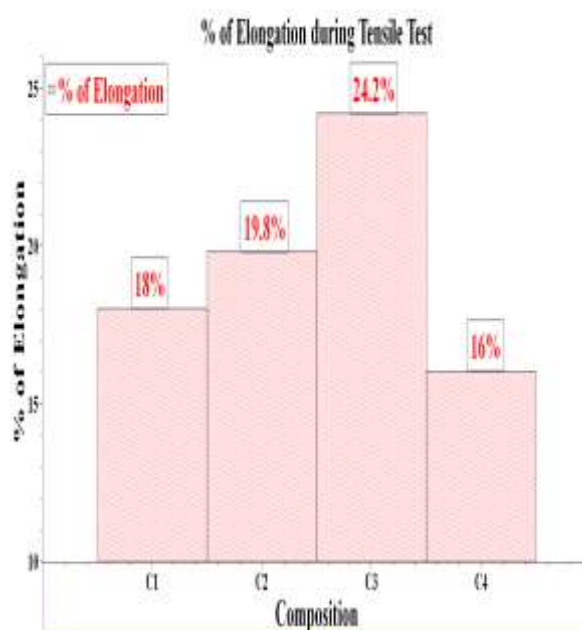


Fig 6. Percentage of Elongation with different Specimen

3.4 Evaluation of Fatigue behaviour:

Table.5 Fatigue Test Data

Compositio n	Specimen no	load (kg)	No of Cycle s (N)	No of cycles completed	Stress in MPa	Failure Mode
Pure AA7075	1	70	10 ⁵	15468	44.114	No Failure
	2	80		12456	44.267	No Failure
	3	90		8546	48.257	Failed
	4	100		3658	52.492	Failed
	5	110		524	53.657	Failed
	6	120		97	54.785	Failed
AA7075+2 wt.% Si3N4+0.5	1	70	10 ⁵	15986	51.480	No Failure
	2	80		14680	51.697	No Failure
	3	90		7850	57.824	Failed
	4	100		4320	59.372	Failed

wt.% HfC+2	5	110		758	59.878	Failed
wt.% MoS2	6	120		104	60.874	Failed
AA7075+5	1	70		17653	52.421	No Failure
wt.%	2	80		15784	52.652	No Failure
Si3N4+1.25	3	90	10 ⁵	7523	57.890	Failed
wt.%	4	100		4658	62.652	Failed
HfC+3.5	5	110		948	63.669	Failed
wt.% MoS2	6	120		121	64.587	Failed
AA7075+8	1	70		9240	51.890	Failed
wt.%	2	80		5420	54.690	Failed
Si3N4+2	3	90	10 ⁵	958	59.301	Failed
wt.% HfC+5	4	100		452	60.623	Failed
wt.% MoS2	5	110		112	61.785	Failed
	6	120		79	62.440	Failed

Fig.7 shows the S-N curve of low cycle fatigue behaviour. The fatigue life results are shown in Table.5; the results are conjoint with the tensile behaviour results, as the reinforcement wt.% increases, there is an increase in stress value, and the predetermined cycles (104) are reached if the load for each composition is changed from higher to lower. Specimen 1 & 2 of composition AA7075+5 wt.% Si₃N₄+1.25 wt.% HfC+3.5 wt.% MoS₂ shows the full life cycles than the other composition specimens; however, the specimens of compositions AA7075+8 wt.% Si₃N₄+2 wt.% HfC+5 wt.% MoS₂ has not reached the maximum Number of cycles due to the arrangement of the interface particles where the load is not transferred correctly to the reinforcements which increase the plastic deformation of the matrix material [26]. As the stress decreases, the fatigue life of the specimen increases. This stress limit is one of the material properties, which shows the fatigue or endurance limit of the material. The S-N curve in Fig.7 indicates the endurance limit of each specimen between the stress and the Number of cycles. The fatigue life is decreased in other specimens and results in failure mode due to the fatigue cracks are developed on the specimen surface; most commonly, the crack initiation initially happens on the subsurface of the interior [27].

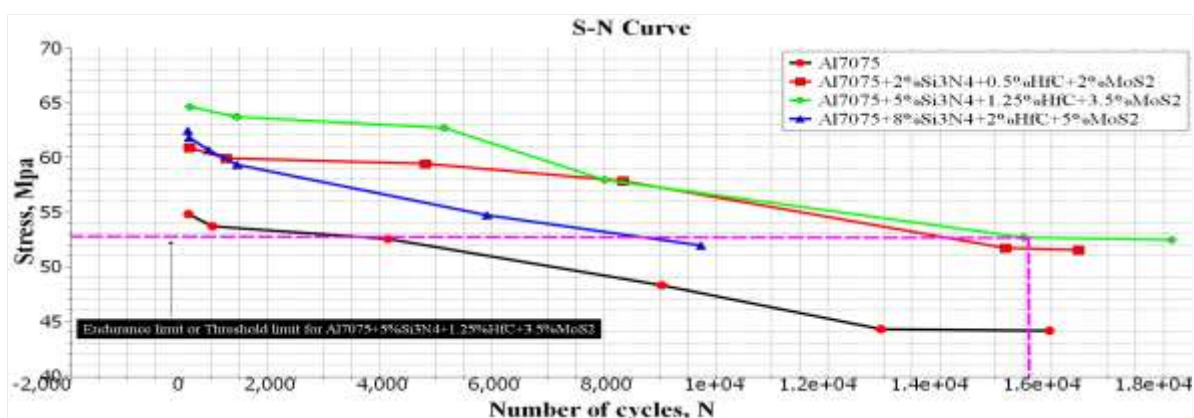


Fig 7. S-N curve of Fatigue Test

3.5 Evaluation of Scanning Electron Microscopy:

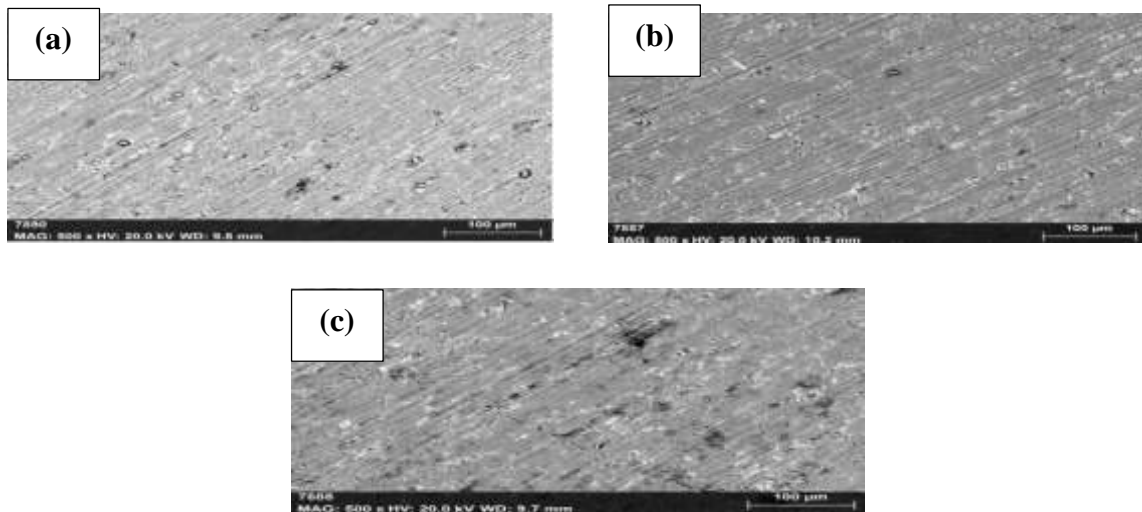


Fig 8. SEM of sintered samples **a)** Al7075-0wt.% **b)** Al7075+2wt.% Si₃N₄+0.5 wt.% HfC+ 2 wt.% MoS₂, **c)** Al7075+5 wt.% Si₃N₄+1.25 wt.% HfC+3.5 wt.% MoS₂ and **d)** Al7075+8 wt.% Si₃N₄+2 wt.% HfC+ 5 wt.% MoS₂

Generally, the casting defects can be seen in the Al7075 Composites, such as cracks and porosity. However, adding the reinforcements, the SEM image shows that at 2 Si₃N₄-0.5 HfC- 2 MoS₂ wt.% and Al-5 Si₃N₄-1.25 HfC- 3.5 MoS₂ wt.% the particles were uniformly distributed and almost homogeneously in the matrix, this is due to the presence of the ceramic particles with the base alloy which are thermodynamically stable and produce pure interfaces which increase the load and bearing capabilities shown in Fig. 8a & 8b, whereas in the Al-8 Si₃N₄-2 HfC- 5 MoS₂ wt.% in Fig. 8c shows some porosity and cracks due to the thermodynamically unstable ceramic particles, which results in unpleasant compounds [25]. The (EDS) spectrum analysis in Fig 9 & Fig 10 shows the presence of Silicon nitride, Hafnium carbide, and molybdenum Disulphide reinforcements with the base alloy wt.% added for the composition 2 Si₃N₄-0.5 HfC- 2 MoS₂ wt.% and Al-5 Si₃N₄-1.25 HfC- 3.5 MoS₂ wt.%. Table 6 shows the weight percentage of the elements present in the MMC's for the composition C3.



Fig 9. EDS Spectrum of the hybrid composites (Al7075 with 2wt.% Si₃N₄, 0.5wt.% HfC, 2wt.% MoS₂)

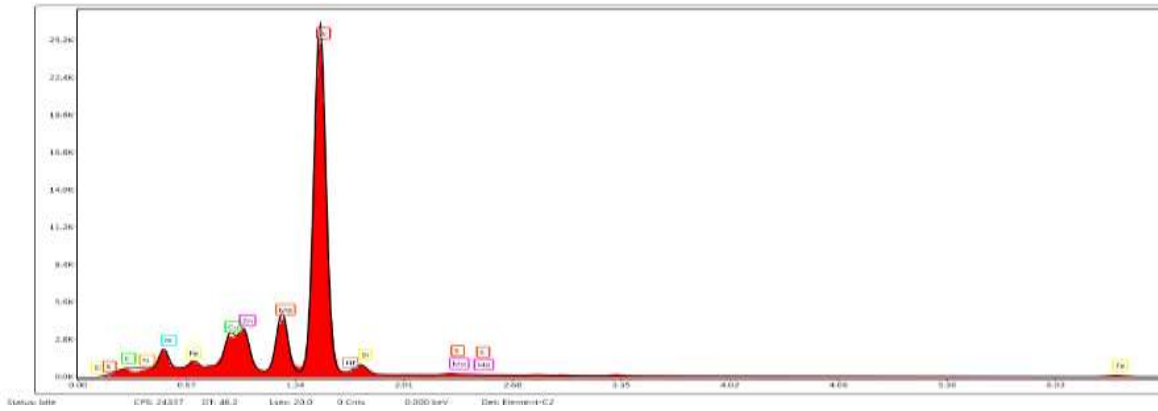


Fig 10. EDS Spectrum of the hybrid composites (Al7075 with 5wt.% Si₃N₄, 1.25wt.% HfC, 3.5wt.% MoS₂)

Table.6 C3 - Composition Element percentage

Element	C K	N K	O K	Fe L	Cu L	Zn L	Mg K	Al K	Hf M	Si K	S K
Weight %	20.49	1.51	15.14	0.41	1.97	4.15	4.06	50.06	0.62	1.27	0.32
Atomic %	34.51	2.18	19.15	0.15	0.63	1.28	3.38	37.53	0.07	0.92	0.2

3.6 Evaluation of Fractography:

The SEM fractography images after tensile tests are shown in Fig 11 (a-d). The fracture surface of base alloy Al 7075 without adding reinforcements shows a large size dimple, which indicates the ductile fracture. In contrast, the dimple sizes are getting finer while adding the reinforcements, so it has a mixed fracture mode, whereas during the Al-5 Si₃N₄-1.25 HfC- 3.5 MoS₂ wt.% the dimple formation is less and interfacial bonding between the base alloy and the reinforcements are very good. However, in the Al-8 Si₃N₄-2 HfC- 5 MoS₂, the composites have produced more particulate cracks, and it has a large amount of brittle nature, which result in less mechanical properties and also due to the presence of more hard ceramic particles in the Al7075 matrix.

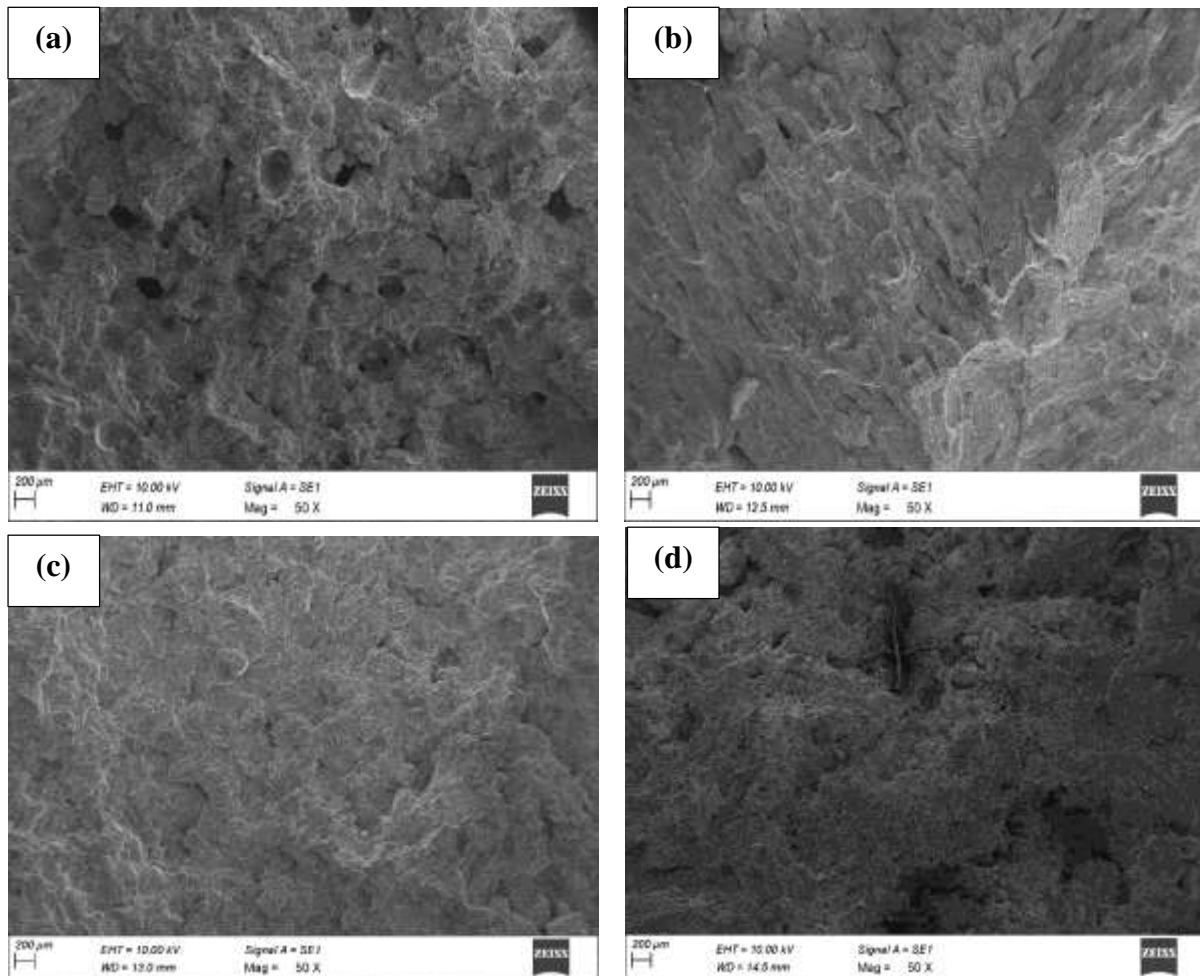


Fig 11. SEM fractography images Tensile Fracture samples **a)** Al7075-0wt.% **b)** Al7075+2wt.% Si_3N_4 +0.5 wt.% HfC+ 2 wt.% MoS_2 , **c)** Al7075+5 wt.% Si_3N_4 +1.25 wt.% HfC+3.5 wt.% MoS_2 and **d)** Al7075+8 wt.% Si_3N_4 +2 wt.% HfC+ 5 wt.% MoS_2

4. Conclusion

The mechanical behaviour testing results of AL7075 reinforced with Si_3N_4 , HfC, and MoS_2 provide the following conclusions.

The microhardness of the hybrid composites materials is increased from 75.4 VHN to 156.8 VHN with an increase of reinforcements from 2 wt.% Si_3N_4 , 0.5 wt.% HfC, 2wt.% MoS_2 to 8 wt.% Si_3N_4 , 2 wt.% HfC, 5 wt.% MoS_2 .

The tensile test of the hybrid composites materials having reinforcements of 5wt.% Si_3N_4 , 1.25wt.%HfC, 3.5wt.% MoS_2 shows a higher value than the base alloy. However, more reinforcements added will result in brittle fracture due to the dislocation of the particles at the interface.

The fatigue test is found to be increasing as the wt.% of the reinforcements increases. The following results show that the composition 5wt.% Si_3N_4 , 1.25wt.%HfC, and 3.5wt.% MoS_2 have higher stress values than other specimens due to the fine grain size for better resistance.

The SEM analysis of the fabricated samples shows the uniform distribution of the reinforcements. When the reinforcements are exceeded above 5wt.% Si₃N₄, 1.25wt.% HfC, 3.5wt.% MoS₂, there occurs thermal instability between the base alloy and reinforcements, which results in cracks and porosity.

The Fractography SEM of tensile tests showed minor dimples and porosity when the reinforcements were added, resulting in ductile and brittle. However, when the reinforcements exceed above 5wt.% Si₃N₄, 1.25wt.% HfC, 3.5wt.% MoS₂, the crack propagation happens due to the sharp edges of heavy ceramic particles.

References:

1. Sambathkumar, M., Navaneethakrishnan, P., Ponappa, K., & Sasikumar, K. S. K. (2017). Mechanical and Corrosion Behavior of Al7075 (Hybrid) Metal Matrix Composites by Two Step Stir Casting Process. *Latin American Journal of Solids and Structures*, 14(2), 243–255.
2. Gunasekaran, T., Vijayan, S. N., Prakash, P., & Satishkumar, P. (2020). Mechanical properties and characterization of Al7075 aluminum alloy based ZrO₂ particle reinforced metal-matrix composites. *Materials Today: Proceedings*, S2214785320387204.
3. Imran, M., Khan, A. R. A., Megeri, S., & Sadik, S. (2016). Study of hardness and tensile strength of Aluminium-7075 percentage varying reinforced with graphite and bagasse-ash composites. *Resource-Efficient Technologies*, 2(2), 81–88.
4. Kumar, A., Patnaik, A., & Bhat, I. K. (2018). Effect of titanium metal powder on thermo-mechanical and sliding wear behavior of Al7075/Ti alloy composites for gear application. *Materials Today: Proceedings*, 5(9), 16919–16927.
5. Li, L., Li, R., Yuan, T., Chen, C., Zhang, Z., & Li, X. (2020). Microstructures and tensile properties of a selective laser melted Al–Zn–Mg–Cu (Al7075) alloy by Si and Zr microalloying. *Materials Science and Engineering: A*, 787, 139492.
6. Kumar Gupta, T., Kumar Srivastava, A., & Shankar Srivastava, V. (2021). Microstructural and tensile behaviour of hybrid MMC Al7075/ SiC/B₄C produced by mechanical stir casting. *Materials Today: Proceedings*, 47, 4107–4113.
7. Kumar, S. A., Prabhu Kumar, A., Balu Naik, B., & Ravi, B. (2018). Production and investigation on Mechanical Properties of TiC reinforced Al7075 MMC. *Materials Today: Proceedings*, 5(9), 17924–17929.
8. Kumar, N., & G., I. (2021). A review on tribological behaviour and mechanical properties of Al/ZrO₂ metal matrix nano composites. *Materials Today: Proceedings*, 38, 2649–2657.
9. Raja, T., Prabhakaran, R., Praveen Kumar, D., & Sathish, D. (2021). Mechanical and tribological characteristics of AL7075/MWCNT, B₄C & MoS₂ hybrid metal matrix composites. *Materials Today: Proceedings*, S2214785321046472.
10. Suhael Ahmed, S., & Girisha, H. N. (2021). Experimental investigations on mechanical properties of Al7075/TiB₂/Gr hybrid composites. *Materials Today: Proceedings*, 46, 6041–6044.
11. Gosavi, S. V., & Jaybhaye, M. D. (2021). Microstructural studies on aluminium metal matrix composite (Al7075-SiC) fabricated through stir casting process. *Materials Today: Proceedings*, 39, 1412–1416.

12. Surya, M. S., & Prasanthi, G. (2021). Manufacturing, microstructural and mechanical characterization of powder metallurgy processed Al7075/SiC metal matrix composite. *Materials Today: Proceedings*, 39, 1175–1179.
13. Sethi, D., Acharya, U., Medhi, T., Shekhar, S., & Roy, B. S. (2021). Microstructural and mechanical property of friction stir welded Al7075/TiB₂ aluminium matrix composite. *Materials Today: Proceedings*, 46, 9180–9186.
14. Lakshmanan, M., Selwin Rajadurai, J., Chakkravarthy, V., & Rajakarunakaran, S. (2021). Tribological investigations on h-BN/NiTi inoculated Al7075 composite developed via ultrasonic aided squeeze casting. *Materials Letters*, 285, 129113.
15. Rao, T. B. (2021). Microstructural, mechanical, and wear properties characterization and strengthening mechanisms of Al7075/SiCnp composites processed through ultrasonic cavitation assisted stir-casting. *Materials Science and Engineering: A*, 805, 140553.
16. Bharath, L., Sreenivasa Reddy, M., Girisha, H. N., & Balakumar, G. (2021). Optimization of ductility and yield strength on Al2024/B 4 C composite material using Taguchi Technique. *IOP Conference Series: Materials Science and Engineering*, 1055(1), 012117.
17. Raghuvaran, P., Baskaran, J., Aagash, C., Ganesh, A., & Gopi Krishna, S. (2021). Evaluation of mechanical properties of Al7075-SiC composites fabricated through stir casting technique. *Materials Today: Proceedings*, 45, 1914–1918.
18. Surya, V. R., Kumar, K. M. V., Keshavamurthy, R., Ugrasen, G., & Ravindra, H. V. (2017). Prediction of Machining Characteristics using Artificial Neural Network in Wire EDM of Al7075 based In-situ Composite. *Materials Today: Proceedings*, 4(2), 203–212.
19. Soni, S., & Thomas, B. (2020). Microstructure, mechanical properties and machinability studies of Al7075/SiC/h-BN hybrid nanocomposite fabricated via ultrasonic-assisted squeeze casting. *FME Transactions*, 48(3), 532–542.
20. Pasha, S. S., Imran, M., & Harish, S. N. (2020). Wear rate and hardness characteristics of Al7075/kyanite (Al₂SiO₅) composites. *Materials Today: Proceedings*, 26, 922–928.
21. Javdani, A., & Daei-Sorkhabi, A. H. (2018). Microstructural and mechanical behavior of blended powder semisolid formed Al7075/B 4 C composites under different experimental conditions. *Transactions of Nonferrous Metals Society of China*, 28(7), 1298–1310.
22. Azimi, A., Shokuhfar, A., & Nejadseyfi, O. (2015). Mechanically alloyed Al7075–TiC nanocomposite: Powder processing, consolidation and mechanical strength. *Materials & Design (1980-2015)*, 66, 137–141.
23. Mistry, J. M., & Gohil, P. P. (2019). Experimental investigations on wear and friction behaviour of Si₃N₄p reinforced heat-treated aluminium matrix composites produced using electromagnetic stir casting process. *Composites Part B: Engineering*, 161, 190–204.
24. Devaganesh, S., Dinesh Kumar, P. K., Venkatesh, N., & Balaji, R. (2020). Study on the mechanical and tribological performances of hybrid SiC-Al7075 metal matrix composites. *Journal of Materials Research and Technology*, 9(3), 3759–3766.
25. Ma, K., Wen, H., Hu, T., Topping, T. D., Isheim, D., Seidman, D. N., Lavernia, E. J., & Schoenung, J. M. (2014). Mechanical behavior and strengthening mechanisms in ultrafine grain precipitation-strengthened aluminum alloy. *Acta Materialia*, 62, 141–155.
26. Esmaeili, A., Shaeri, M. H., Noghani, M. T., & Razaghian, A. (2018). Fatigue behavior of AA7075 aluminium alloy severely deformed by equal channel angular pressing. *Journal of Alloys and Compounds*, 757, 324–332.

27. Zhao, T., & Jiang, Y. (2008). Fatigue of 7075-T651 aluminum alloy. *International Journal of Fatigue*, 30(5), 834–849.
28. Ramkumar, K. R., Bekele, H., & Sivasankaran, S. (2015). Experimental Investigation on Mechanical and Turning Behavior of Al 7075/ x % wt. TiB₂ -1% Gr In Situ Hybrid Composite. *Advances in Materials Science and Engineering*, 2015, 1–14.

Authors Profile



FIRST AUTHOR: N.UMMAL SALMAAN, B.E.,M.S,(Ph.D) Bachelor degree in Mechanical Engineering and Master’s degree in Automotive from University of Toledo, Ohio, USA.
Working Experience: Assistant professor for past 7 Years, currently working at Aksum University, Ethiopia. Research Scholar: Karunya Institute of Technology and Sciences, Coimbatore, Tamilnadu – 641114, India. Research Field: Automotive Composite Materials, Technical Paper Publications: 06



SECONDAUTHOR: DR.D.S.ROBINSONSMART.,M.E.,Phd, Professor, Department of Mechanical Engineering, Karunya Institute of Technology and Sciences, Coimbatore, Tamilnadu – 641114, India. Qualification: B.E, M.E & Ph.d, Experience: Teaching and Research: 28 years, Technical Paper Publications: 83, Awards: 03, Research work: Abrasive Jet Machining and Materials



THIRD AUTHOR: DR. S. ANTONY RAJA., M.E., Phd, Associate Professor, Department of Mechanical Engineering, Karunya Institute of Technology and Sciences, Coimbatore, Tamilnadu – 641114, India. Qualification: B.E, M.E & Ph.d, Experience: Teaching and Research: 15 years, Technical Paper Publications: 13, Research Area: Renewable Energy and Materials.